

AD-760 130

**THE ABSORPTION BY H₂O BETWEEN 1630 AND 2245/cm
(6.13 - 4.44 MICROMETER)**

Darrell E. Burch, et al

Philco-Ford Corporation

Prepared for:

**Air Force Cambridge Research Laboratories
Defense Advanced Research Projects Agency**

January 1973

DISTRIBUTED BY:

NTIS

**National Technical Information Service
U. S. DEPARTMENT OF COMMERCE
5285 Port Royal Road, Springfield Va. 22151**

AD 760130

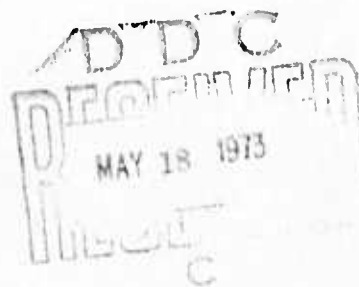
THE ABSORPTION BY H_2O BETWEEN 1630 AND 2245 cm^{-1}
(6.13 - 4.44 μm)

by

Darrell E. Burch
David A. Gryvnak
John D. Pembroke

Philco-Ford Corporation
Aeronutronic Division
Ford Road
Newport Beach, California 92663

Contract No. F19628-73-C-0011
Project No. 8692



Semi-Annual Technical Report No. 1

January 1973

Contract Monitor: Robert A. McClatchey
Optical Physics Laboratory

Approved for public release; distribution unlimited

Sponsored by
Defense Advanced Research Projects Agency
ARPA Order No. 1366
Monitored by
AIR FORCE CAMBRIDGE RESEARCH LABORATORIES
AIR FORCE SYSTEMS COMMAND
UNITED STATES AIR FORCE
BEDFORD, MASSACHUSETTS 01730

Reproduced by
NATIONAL TECHNICAL
INFORMATION SERVICE
U S Department of Commerce
Springfield VA 22151

SECTION 1	
WTS	Whole Section <input checked="" type="checkbox"/>
TS	Full Section <input type="checkbox"/>
DISCONTINUED	<input type="checkbox"/>
SECTION 2	
BY	
IDENTIFICATION/CLASSIFICATION CODES	
100	100
A	

ARPA Order No. 1366

Program Code No. 2E50

Contractor: Philco-Ford Corporation

Effective Date of Contract: 15 March 1973

Contract No. F19628-73-C-0011

Principal Investigator and Phone No.

Dr. Darrell E. Burch/714 640-1500

AFCRL Project Scientist and Phone No.

Dr. Robert A. McClatchey/617 861-3224

Qualified requestors may obtain additional copies from the
Defense Documentation Center.
All others should apply to the National Technical Information Service.

UNCLASSIFIED

Security Classification

DOCUMENT CONTROL DATA - R & D

Security classification of title, body of abstract and indexing annotation must be entered when the overall report is classified.

1. ORIGINATING ACTIVITY (Corporate author) Philco-Ford Corporation Aeronutronic Division Newport Beach, California 92663		2a. REPORT SECURITY CLASSIFICATION Unclassified	
3. REPORT TITLE THE ABSORPTION BY H_2O BETWEEN 1630 AND 2245 cm^{-1} (6.13 - 4.44 μm)		2b. GROUP	
4. DESCRIPTIVE NOTES (Type of report and inclusive dates) Scientific. Interim.			
5. AUTHOR(S) (First name, middle initial, last name) Darrell E. Burch David A. Gryvnak John D. Pembrook			
6. REPORT DATE January 1973	7a. TOTAL NO. OF PAGES 28	7b. NO. OF REFS 15	
8a. CONTRACT OR GRANT NO. F19628-73-C-0011 ARPA Order No. 1366		9a. ORIGINATOR'S REPORT NUMBER(S) U-5090 Semi-Annual Technical Report No. 1	
b. Project, Task, Work Unit Nos. 8692 n/a n/a		9b. OTHER REPORT NO(S) (Any other numbers that may be assigned this report)	
c. DoD Element 62301D		AFCRL-TR-73-0092	
d. DoD Subelement n/a			
10. DISTRIBUTION STATEMENT A - Approved for public release; distribution unlimited.			
11. SUPPLEMENTARY NOTES This research was sponsored by the Defense Advanced Research Projects Agency.		12. SPONSORING MILITARY ACTIVITY Air Force Cambridge Research Laboratories L. G. Hanscom Field (OP) Bedford, Massachusetts 01730	
13. ABSTRACT The absorption by samples of H_2O and $H_2O + N_2$ has been studied between 1630 and 2245 cm^{-1} . Spectral curves of transmittance have been obtained for samples covering a wide range of pressures with temperatures between 308 K and 428 K. The emphasis has been on continuum absorption in approximately 30 narrow windows where most of the absorption results from lines centered more than 1 cm^{-1} from the point of absorption. Comparison of the results with calculated values based on published line parameters indicates that the extreme wings of H_2O lines absorb more than Lorentz-shaped lines of the same intensity and half-width. The continuum absorption decreases with increasing temperature at a faster rate than is predicted by simple theory on line shapes.			

DD FORM 1473
1 NOV 68UNCLASSIFIED
Security Classification

14 KEY WORDS	LINK A		LINK B		LINK C	
	ROLE	WT	ROLE	WT	ROLE	WT
H ₂ O Atmospheric Transmission Absorption Continuum Absorption						

ja

THE ABSORPTION BY H_2O BETWEEN 1630 AND 2245 cm^{-1}
(6.13 - 4.44 μm)

by

Darrell E. Burch
David A. Gryvnak
John D. Pembroke

Philco-Ford Corporation
Aeronutronic Division
Ford Road
Newport Beach, California 92663

Contract No. F19628-73-C-0011
Project No. 8692

Semi-Annual Technical Report No. 1

January 1973

Contract Monitor: Robert A. McClatchey
Optical Physics Laboratory

Approved for public release; distribution unlimited

Sponsored by
Defense Advanced Research Projects Agency
ARPA Order No. 1366

Monitored by
AIR FORCE CAMBRIDGE RESEARCH LABORATORIES
AIR FORCE SYSTEMS COMMAND
UNITED STATES AIR FORCE
BEDFORD, MASSACHUSETTS 01730

ib

TABLE OF CONTENTS

<u>Section</u>	<u>Page</u>
1 INTRODUCTION.	I-i
Background.	I-1
Symbols, Units, and Definitions	I-2
2 SPECTRAL TRANSMITTANCE FROM 1860 TO 2230 cm^{-1}	2-1
Fig. 2-1, Spectral curves of transmittance from 1860 to 1953 cm^{-1} for 2 pure samples of H_2O	2-2
Fig. 2-2, Spectral curves of transmittance from 1953 to 2049 cm^{-1} for 2 pure H_2O samples.	2-3
Fig. 2-3, Spectral curves of transmittance from 2049 to 2143 cm^{-1} for 2 pure H_2O samples.	2-4
Fig. 2-4, Spectral curves of transmittance from 2143 to 2243 cm^{-1} for 2 pure H_2O samples.	2-5
Fig. 2-5, Spectral curves of transmittance from 1840 to 1900 cm^{-1} for 3 pure H_2O samples.	2-6
Fig. 2-6, Spectral curve of transmittance from 1900 to 1963 for 3 pure samples of H_2O	2-7
Fig. 2-7, Spectral curve of transmittance from 1963 to 2015 cm^{-1} for 3 pure H_2O samples.	2-8
Fig. 2-8, Spectral curves of transmittance from 2015 to 2080 cm^{-1} for 3 pure H_2O samples.	2-9
Fig. 2-9, Spectral curve of transmittance between 2055 and 2230 cm^{-1}	2-10
Table 2-1, Integrated Absorptance for Pure H_2O	2-11

TABLE OF CONTENTS (Cont.)

<u>Section</u>		<u>Page</u>
3	CONTINUUM ABSORPTION	3-1
	Fig. 3-1, Plots of $(-1/u) \ln T$ vs p at 1978.6 cm^{-1} for H_2O at 352 K and 428 K	3-3
	Table 3-1, Self-Broadening and N_2 -Broadening Coefficients for Different Temperatures.	3-4
	Influence of Nitrogen-Broadening on the Continuum. . .	3-5
	Fig. 3-2, Spectral curves showing a comparison of self-broadened and N_2 -broadened H_2O lines.	3-6
4	REFERENCES	4-1

SECTION 1

INTRODUCTION

Background

The parameters of nearly all of the H_2O lines of significance in the spectral region $1630 - 2245 \text{ cm}^{-1}$ covered by this report have been tabulated by Benedict and Calfee.¹ The tabulated parameters for each line are: line center ν_0 , intensity S , half-width α_0 normalized for air at 1 atm pressure, and the value E'' of the lower energy level involved in the transition. The latter parameter is required in order to calculate the intensity at a temperature different from the standard temperature for which the parameters apply. A combined experimental-theoretical approach was used to determine the parameters. Detailed comparisons with experimental results have not yet been made for all of the individual lines, but there is generally good agreement over intervals several cm^{-1} wide.

Many very strong H_2O lines occur throughout this region, particularly from 1630 to approximately 2000 cm^{-1} , so that the average transmittance is quite low over lower atmospheric paths of a few hundred meters. Although the average transmittance is low, the transmittance may be appreciable in a few "gaps" or narrow "windows" separated by a few cm^{-1} from any very strong lines. The invention of the CO laser has created new interest in these small windows because they coincide with many of the laser lines. Obviously, the performance of the CO laser for communications depends strongly on the atmospheric attenuation. Long et al.² have recently used a CO laser as a radiant energy source to study the transmission of synthetic atmospheres of $\text{H}_2\text{O} + \text{N}_2$ contained in a multiple-pass absorption cell. The emphasis was on several of the narrow windows between approximately 1840 and 1990 cm^{-1} . Long et al have compared many of their experimental results with calculated results based on the Lorentz line

shape and the line parameters published by Benedict et al. In nearly every case, the observed absorptance was greater than the calculated value, sometimes by as much as a factor of 3. Rice,³ using a different method of measuring the attenuation of CO-laser radiant energy by H₂O, has also found poor agreement with calculated results.

The present laboratory investigation was undertaken to check the experimental results of Long et al and to provide additional data from which the continuum absorption could be determined and compared to the calculated results. The discrepancy between the observed and calculated values cannot be explained. It also seems unlikely that errors in the intensities or half-widths are large enough to cause such large errors in the calculated absorptance. Furthermore, it is not probable that the "extra" absorption in this spectral region is due to an H₂O:H₂O dimer as has been suggested as the primary cause of H₂O continuum absorption between 8 and 12 μ m. The most probable explanation involves a deviation from the Lorentz line shape in the extreme wings ($\nu - \nu_0$ greater than approximately 10 cm⁻¹) of the lines. Preliminary analysis of our data indicate that the lack of knowledge about the shapes of the wings of the lines accounts largely for the inability to calculate the absorption reliably. Further analysis of the data, many of which are shown in Sections 2 and 3, will provide additional information on the accuracy of the published values of S and α^0 . It is also anticipated that these data along with other data^{4,5,6,7} on H₂O absorption in windows will provide better insight into the behavior of the wings of lines.

Symbols, Units, and Definitions

At the pressures involved in the present study, the H₂O vapor density is proportional to its partial pressure p so that the absorber thickness u of a sample is given by

$$\begin{aligned} u(\text{molecules/cm}^2) &= 2.69 \times 10^{19} p(\text{atm}) L(\text{cm}) (273/\theta) \\ &= 7.34 \times 10^{21} pL/\theta. \end{aligned} \quad (1-1)$$

The true transmittance that would be observed with infinite resolving power is given by

$$T' = \exp(-u\kappa), \quad \text{or} \quad (-1/u) \ln T' = \kappa, \quad (1-2)$$

where κ is the absorption coefficient. Because of the finite slitwidth of a spectrometer and possible variations in κ with wavenumber due to line structure, the observed transmittance T may differ from T' at the same wavenumber. The quantity T represents a weighted average of T' over the interval passed by the spectrometer.

The intrinsic absorption coefficient due to a single collision-broadened absorption line at a point within a few cm^{-1} of the line center, ν_0 , is probably given adequately by the Lorentz shape:

$$k = \frac{S}{\pi} \frac{\alpha}{(\nu - \nu_0)^2 + \alpha^2} \quad (1-3)$$

The line intensity $S = \int k d\nu$ is essentially independent of pressure for the conditions of the present study. It has been shown^{8,9,10} that for $|\nu - \nu_0|$ greater than a few cm^{-1} , the Lorentz equation may require modification. One method is to employ a factor χ , which is a function of $(\nu - \nu_0)$, so that Eq. (1-3) becomes

$$k = k_L \chi = \frac{S}{\pi} \frac{\alpha \chi}{(\nu - \nu_0)^2 + \alpha^2} \quad (1-4)$$

where k_L denotes the value given by the Lorentz coefficient. The value of χ is approximately equal to unity for small $|\nu - \nu_0|$, but may be quite different for large $|\nu - \nu_0|$. For example, $\chi \ll 1$ for the extreme wings of CO_2 lines, but the data presented below indicates $\chi > 1$ for H_2O lines.

The half-width α is proportional to pressure so that k is, in turn, proportional to pressure in the extreme wings where $|\nu - \nu_0| \gg \alpha$. It follows from Eq. (1-4) that the wing-absorption coefficient C due to the extreme wings of several lines is equal to the sum of all the k 's due to the individual lines and is proportional to pressure, ($C = C^0 p$). Since wing absorption changes slowly with wavenumber, it is frequently called continuum absorption.

Continuum absorption may also arise from dimers,¹¹ such as $\text{H}_2\text{O}:\text{H}_2\text{O}$, or from pressure-induced bands. These two types of continuum have the same pressure dependence as absorption by line wings; therefore, it is not necessary to determine which is the source of the absorption being measured. In the following discussions, we refer to it as wing absorption, although it is possible that some dimer absorption or pressure-induced absorption also occurs. The absorption coefficient due to local lines whose centers occur within a few cm^{-1} of the point of observation is denoted by $\kappa(\text{local})$. This quantity may vary rapidly with wavenumber and depends on pressure as indicated by Eq. (1-3) because of collision-broadening of the absorption lines. At a given wavenumber, there may be absorption by local lines as well as by continuum. Therefore, for a pure H_2O sample, the total absorption coefficient κ in Eq. (1-2) is given by

$$\kappa = \kappa(\text{local}) + C_s = \kappa(\text{local}) + C_s^0 p. \quad (1-5)$$

The normalized continuum coefficient C_s^0 is the value of C_s when $p = 1$ atm. The subscript s denotes self-broadening of the lines. Since u is proportional to pL , $(-L/T)$ due to continuum is proportional to p^2L .

For a mixture of $H_2O + N_2$, such as several of those used in the present study, Eq. (1-5) must be modified to account for the broadening of the H_2O lines by N_2 .

$$\kappa = \kappa(\text{local}) + C_s^0 p + C_{N_2}^0 p_{N_2}, \quad (1-6)$$

where p_{N_2} is the partial pressure of N_2 .

The equivalent pressure P_e given by the following equation is a convenient parameter when dealing with H_2O absorption by mixtures of H_2O in N_2 or in air, which is approximately 80% N_2 :

$$P_e = Bp + p_{N_2} = (B-1)p + P, \quad (1-7)$$

where P is the total pressure. B is the ratio of the self-broadening ability to the broadening ability of N_2 , i.e., $C_s^0/C_{N_2}^0$. We note that P_e approximates P for dilute mixtures of H_2O in N_2 ($p \ll p_{N_2}$). Values of C_s^0 and $C_{N_2}^0$ and B are given in Table 3-1 for selected wavenumbers 2 at different sample temperatures,

SECTION 2

SPECTRAL TRANSMITTANCE FROM 1860 TO 2230 cm^{-1}

Figures 2-1 through 2-4 show spectral curves of transmittance from 1860 to 2243 cm^{-1} for two pure samples of H_2O at a temperature of 322 K. The spectral slitwidth varied from 0.45 to 0.6 cm^{-1} . The two samples were contained in a multiple-pass absorption cell adjusted to 32 passes for a path length of 948.7 meters. After the spectrum of each sample was scanned, a background curve was obtained with the cell evacuated. It was difficult to determine accurately the position of the background curve (corresponding to 100% transmittance) relative to the sample spectrum because of drift during the scanning time of 2-3 hours. In order to position the background curves the following procedure was followed.

Spectral curves were scanned over 8 selected narrow windows for a variety of pure H_2O samples at different pressures. The time required to obtain these data was short enough that the drift in detector signal could be accounted for. The quantity $(-1/u) \ln T$ was plotted against p for the point of maximum transmittance in each window (See Fig. 3-1). These curves were used to modify the background curves relative to the curves for Samples 25 and 18. For wavenumber calibration, more than 55 H_2O absorption lines were identified from a paper by Benedict, Claassen, and Shaw¹² and their positions were determined from a listing by Benedict and Calfee.¹

Figures 2-5 through 2-9 show transmittance spectra for 4 pure H_2O samples at 428 K contained in a multiple-pass cell adjusted for 4 and 32 passes. Background curves were fitted to the sample curves by the method described in the previous paragraph. Table 2-1 lists values of the integrated absorbance $\int A(\nu) d\nu$ for the samples represented in Figs. 2-1 through 2-9, ($A(\nu) = 1 - T(\nu)$).

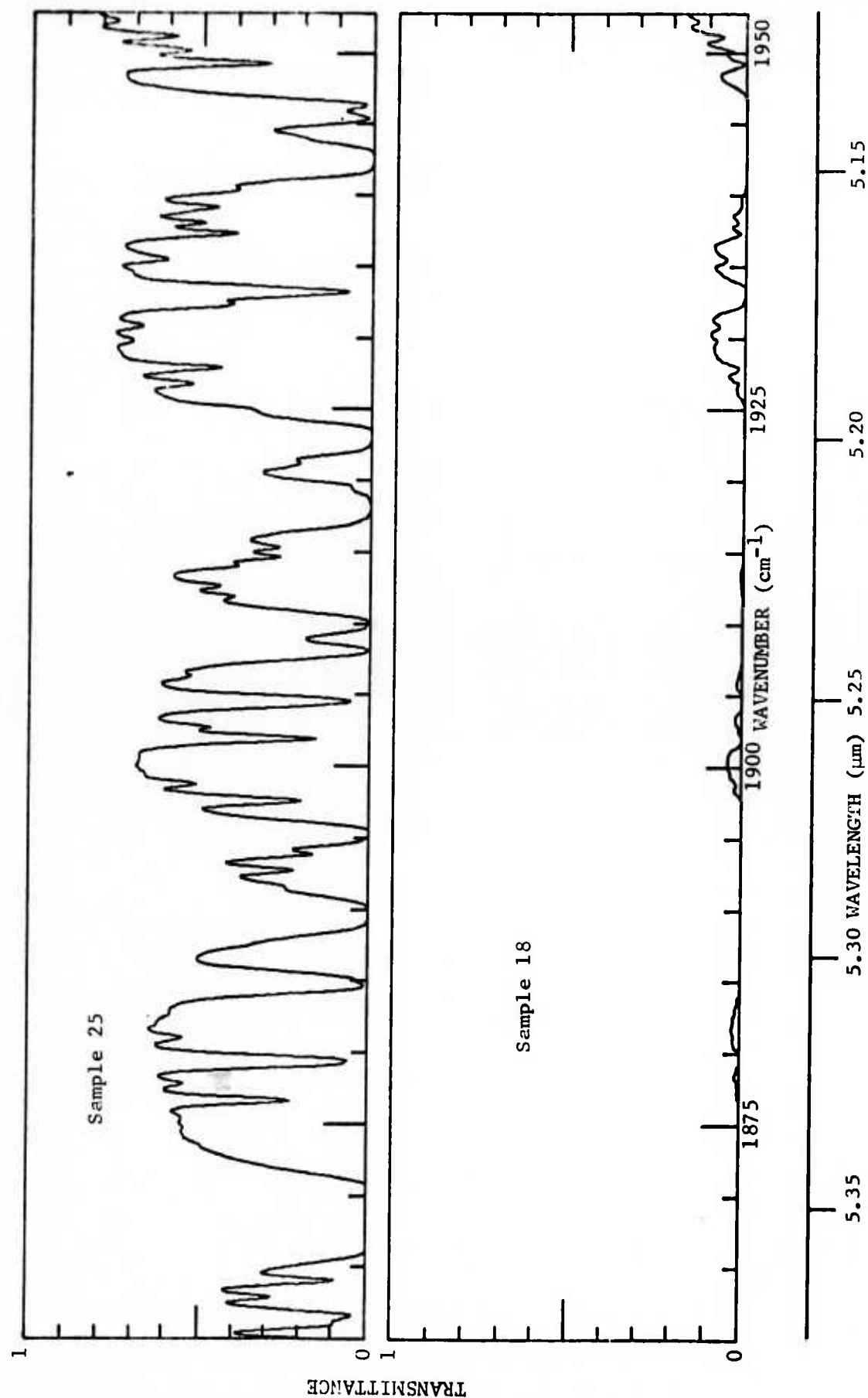


FIG. 2-1. Spectral curves of transmittance from 1860 to 1953 cm⁻¹ for 2 pure samples of H₂O. Spectral slitwidth ≈ 0.45 cm⁻¹.

Sample #	P (atm)	L (cm)	\bar{e} (K)	\bar{u} molecules/cm ²
25	0.0167	94870	322	360 E20
18	0.0526	94870	322	1140 E20

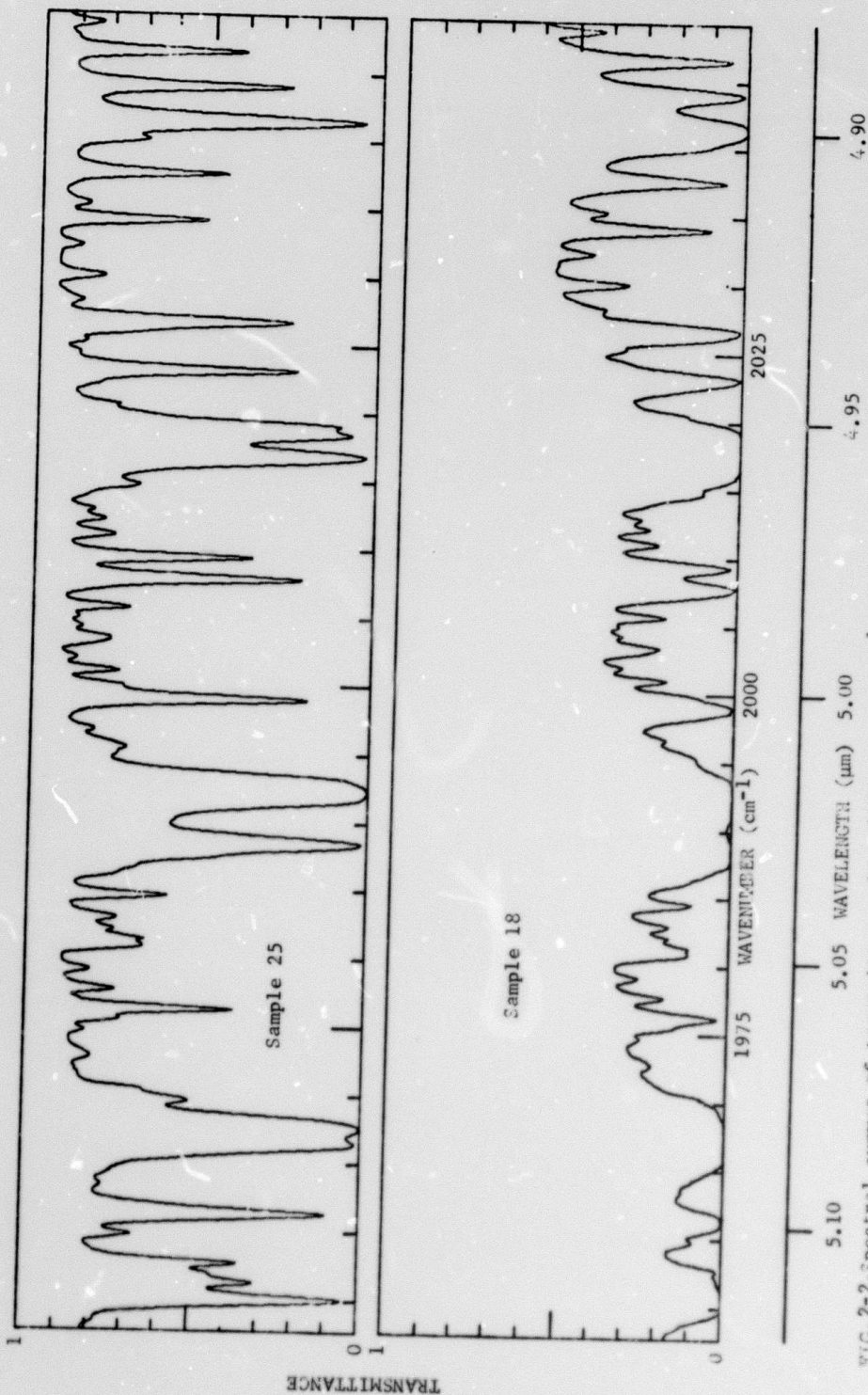


FIG. 2-2. Spectral curves of transmittance from 1953 to 2049 cm⁻¹ for 2 pure H₂O samples. Spectral slitwidth ≈ 0.47 cm⁻¹. Sample parameters are given in Fig. 2-1.

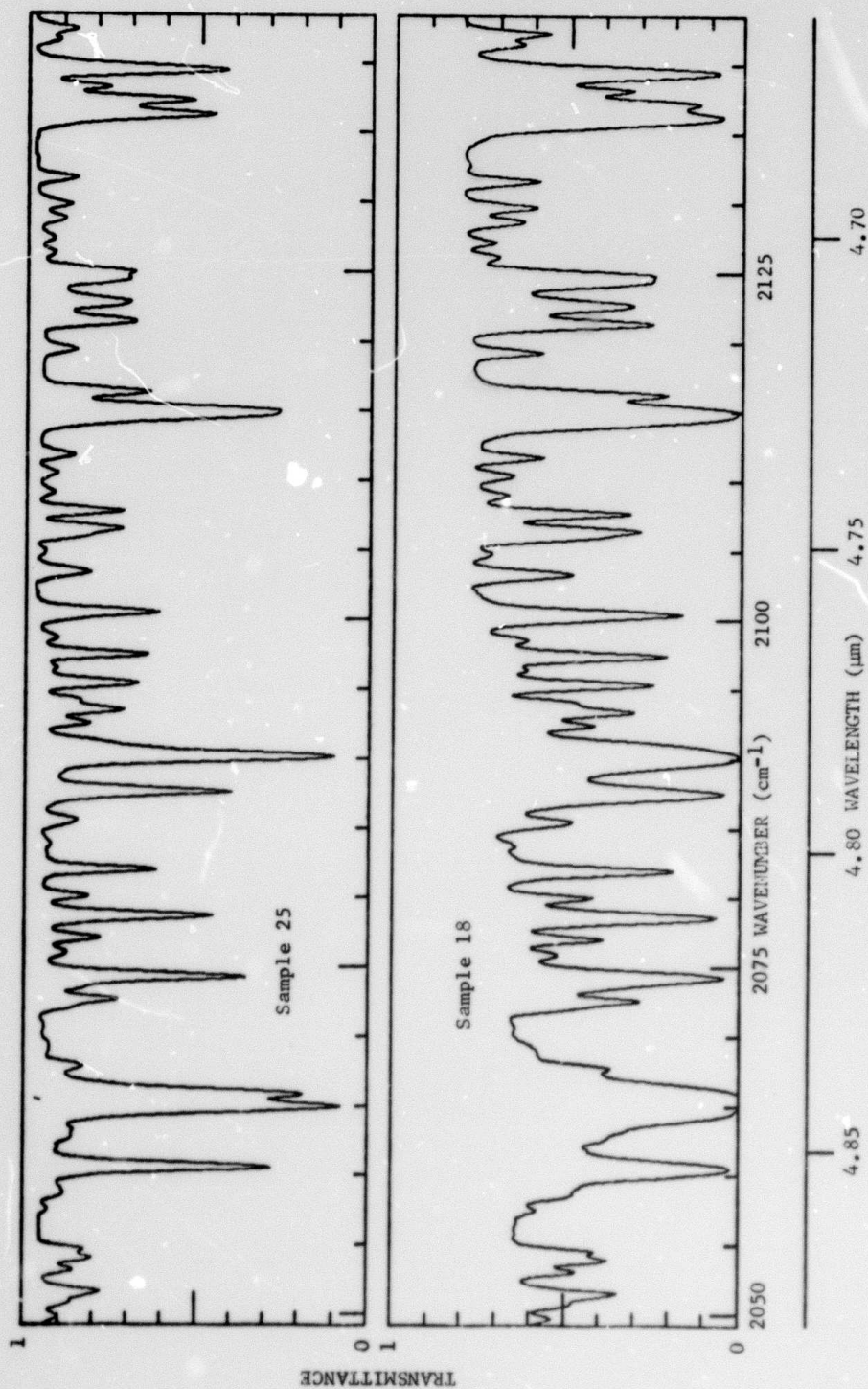


FIG. 2-3. Spectral curves of transmittance from 2049 to 2143 cm^{-1} for 2 pure H₂O samples. Spectral slitwidth = 0.52 cm^{-1} . Sample parameters are given in Fig. 2-1.

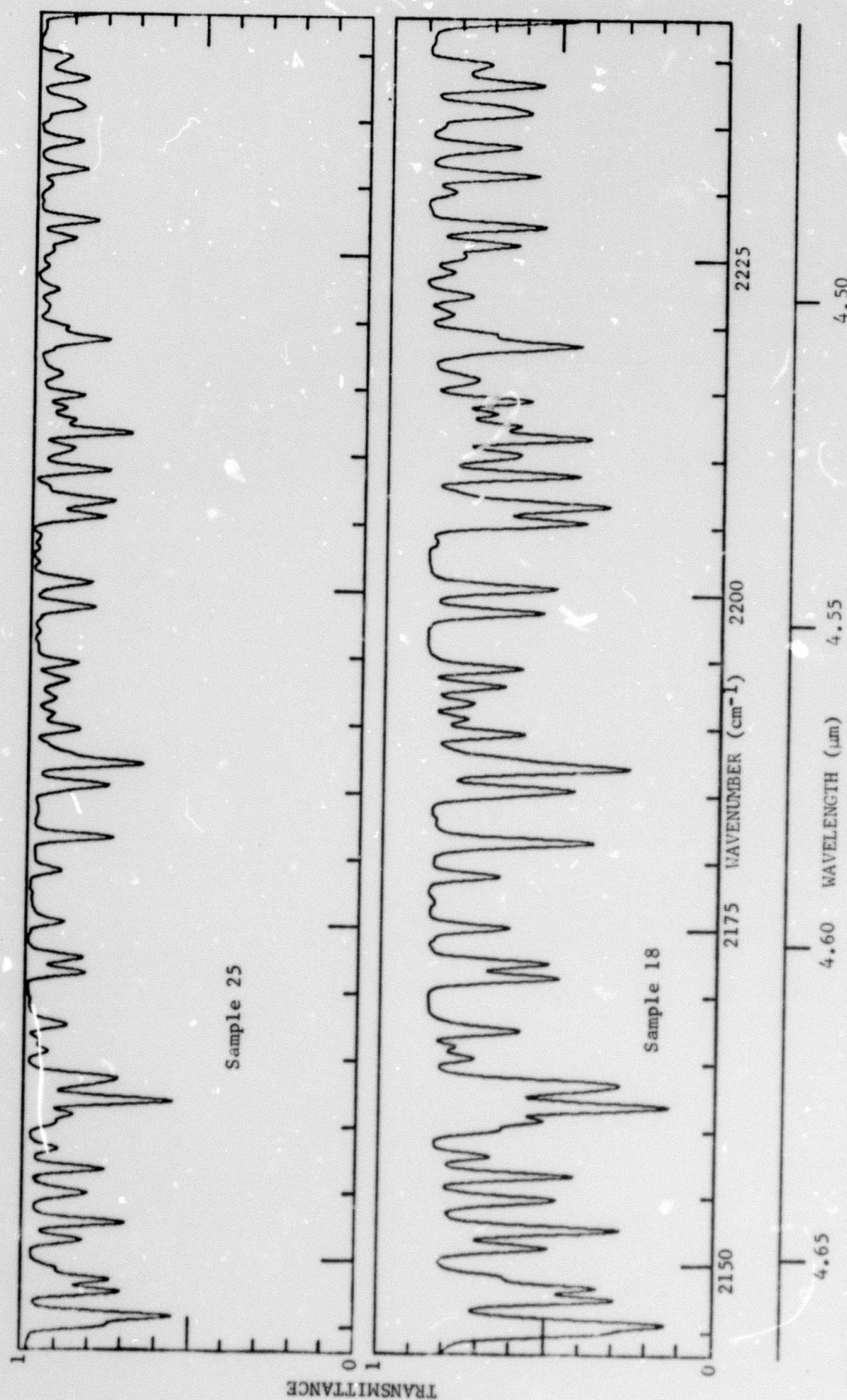


FIG. 2-4. Spectral curves of transmittance from 2143 to 2243 cm^{-1} for 2 pure H_2O samples. Spectral slitwidth $\approx 0.6 \text{ cm}^{-1}$. Sample parameters are given in Fig. 2-1.

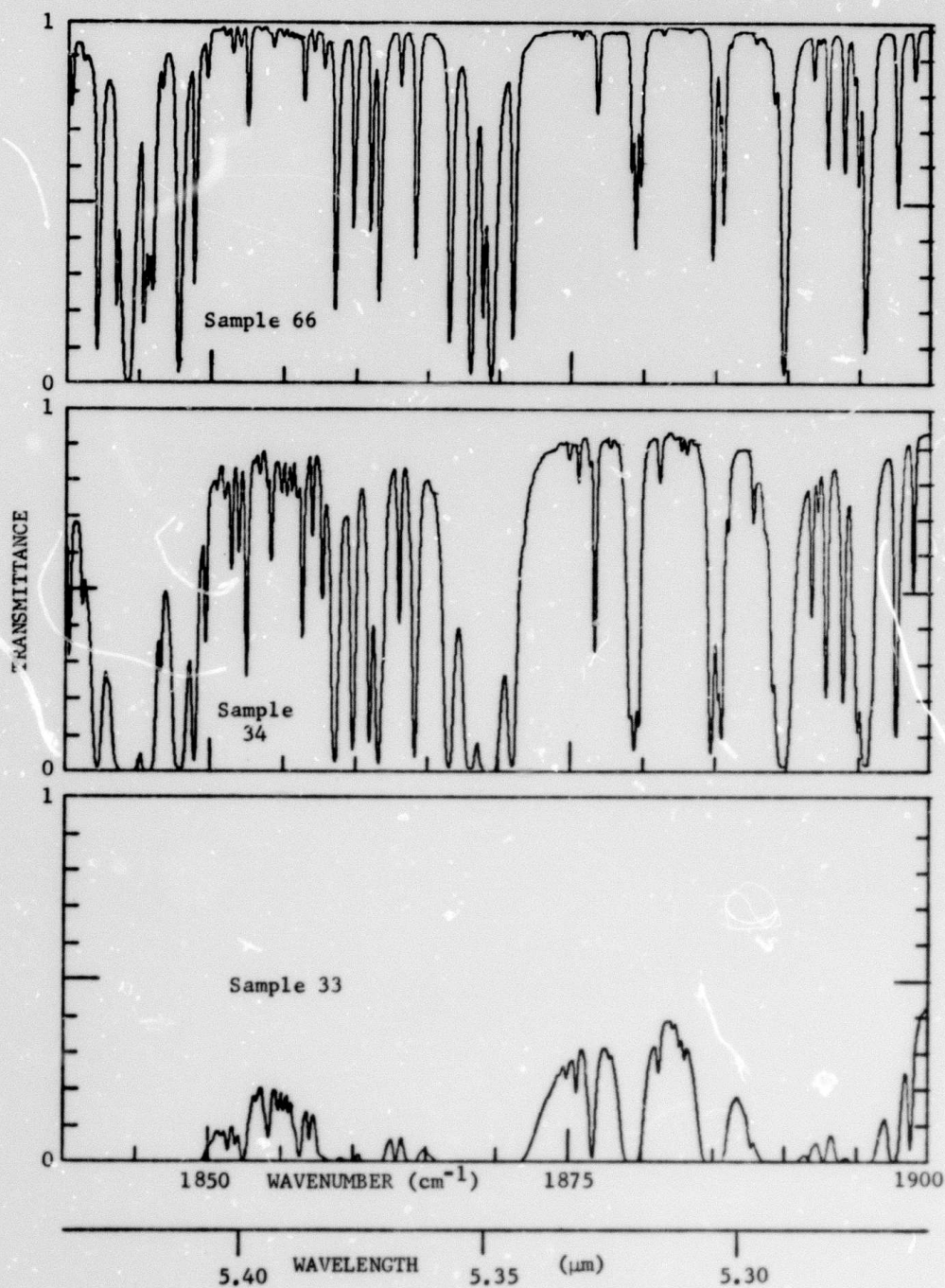


FIG.2-5, Spectral curves of transmittance from 1840 to 1900 cm^{-1} for 3 pure H_2O samples. Spectral slitwidth $\approx 0.18 \text{ cm}^{-1}$.

Sample #	P atm	L cm	θ K	u molecules/ cm^2
66	0.05	416	428	3.58 E20
34	0.05	3291	428	28.2 E20
33	0.2	3291	428	113 E20

2-6

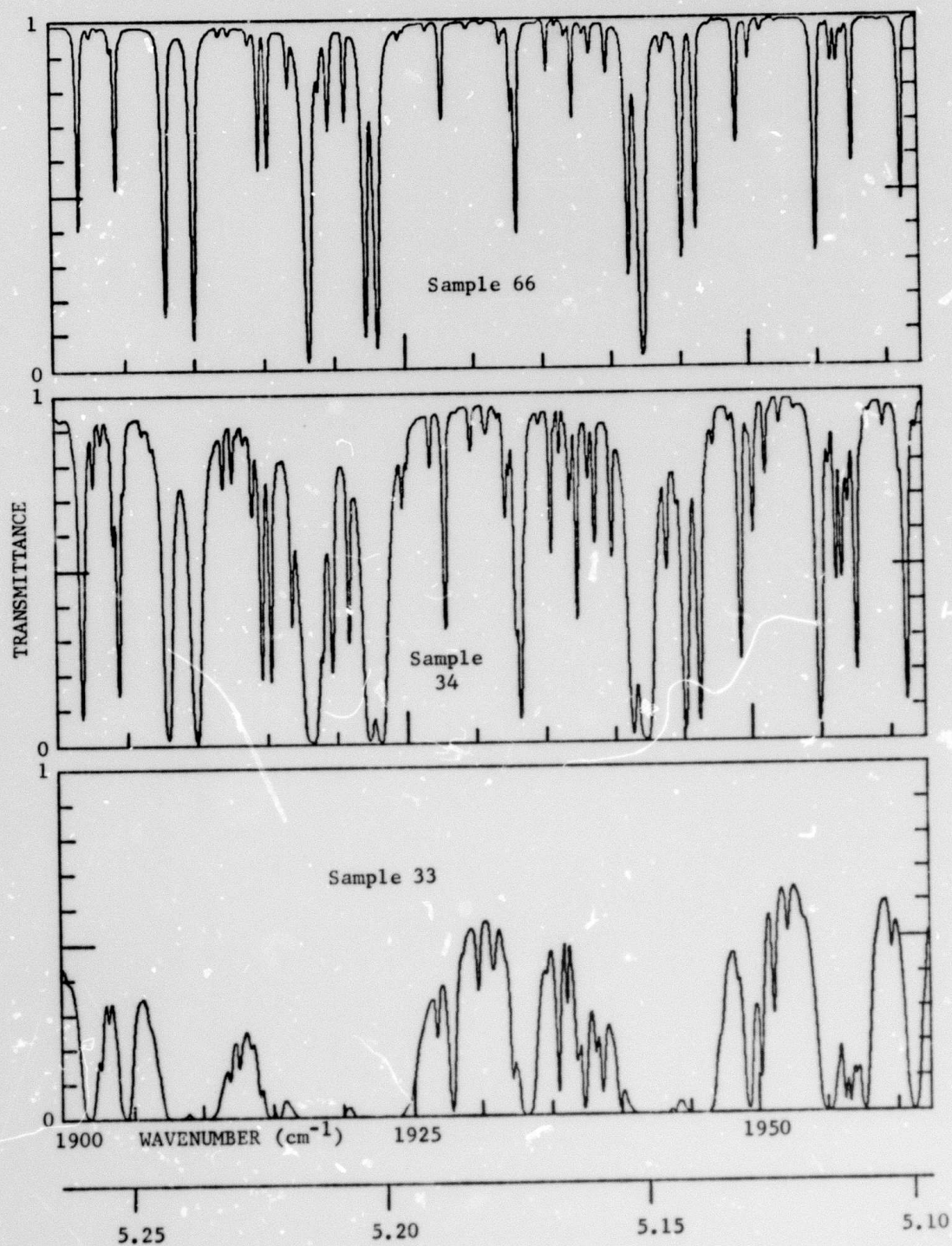


FIG.2-6. Spectral curve of transmittance from 1900 to 1963 for 3 pure samples of H_2O . Spectral slitwidth $\approx 0.19 \text{ cm}^{-1}$. Sample parameters are given in Fig. 2-5.

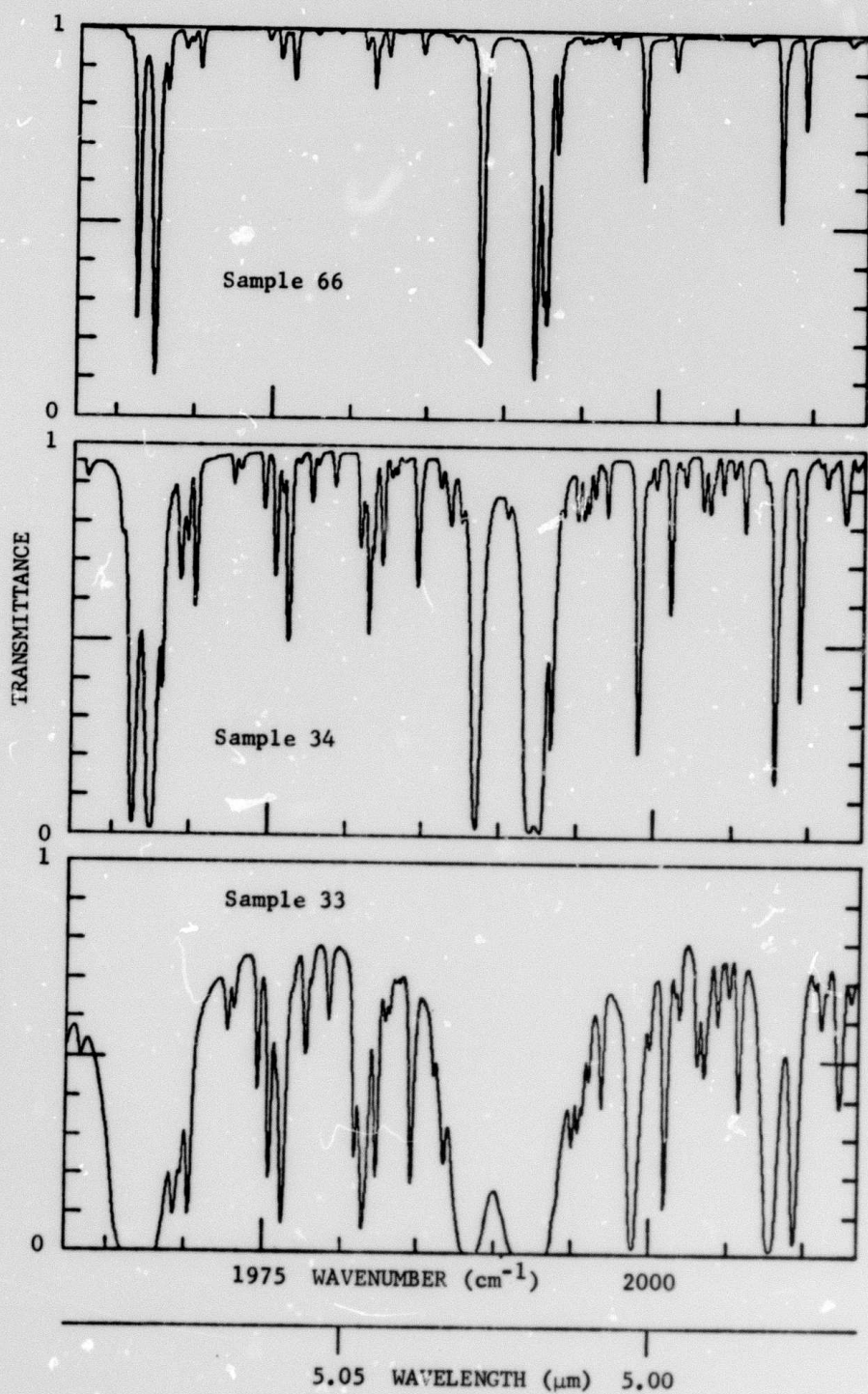


FIG.2-7. Spectral curve of transmittance from 1963 to 2015 cm^{-1} for 3 pure H_2O samples. Spectral slitwidth $\approx 0.19\text{ cm}^{-1}$. Sample parameters are given in Fig. 2-5.

2-8

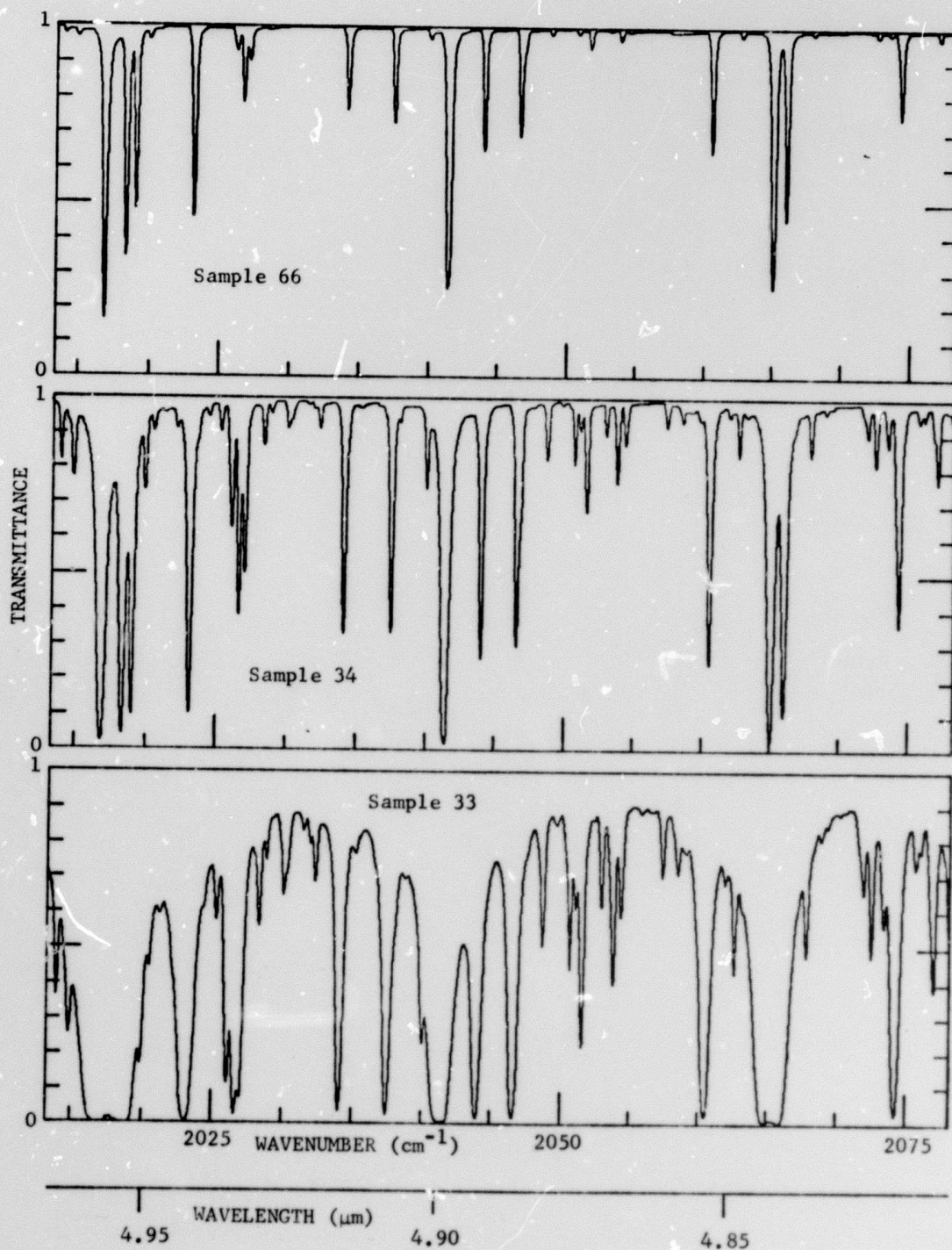


FIG.2-8.Spectral curves of transmittance from 2015 to 2080 cm^{-1} for 3 pure H_2O samples. Spectral slitwidth $\cong 0.20 \text{ cm}^{-1}$. Sample parameters are given in Fig. 2-5.

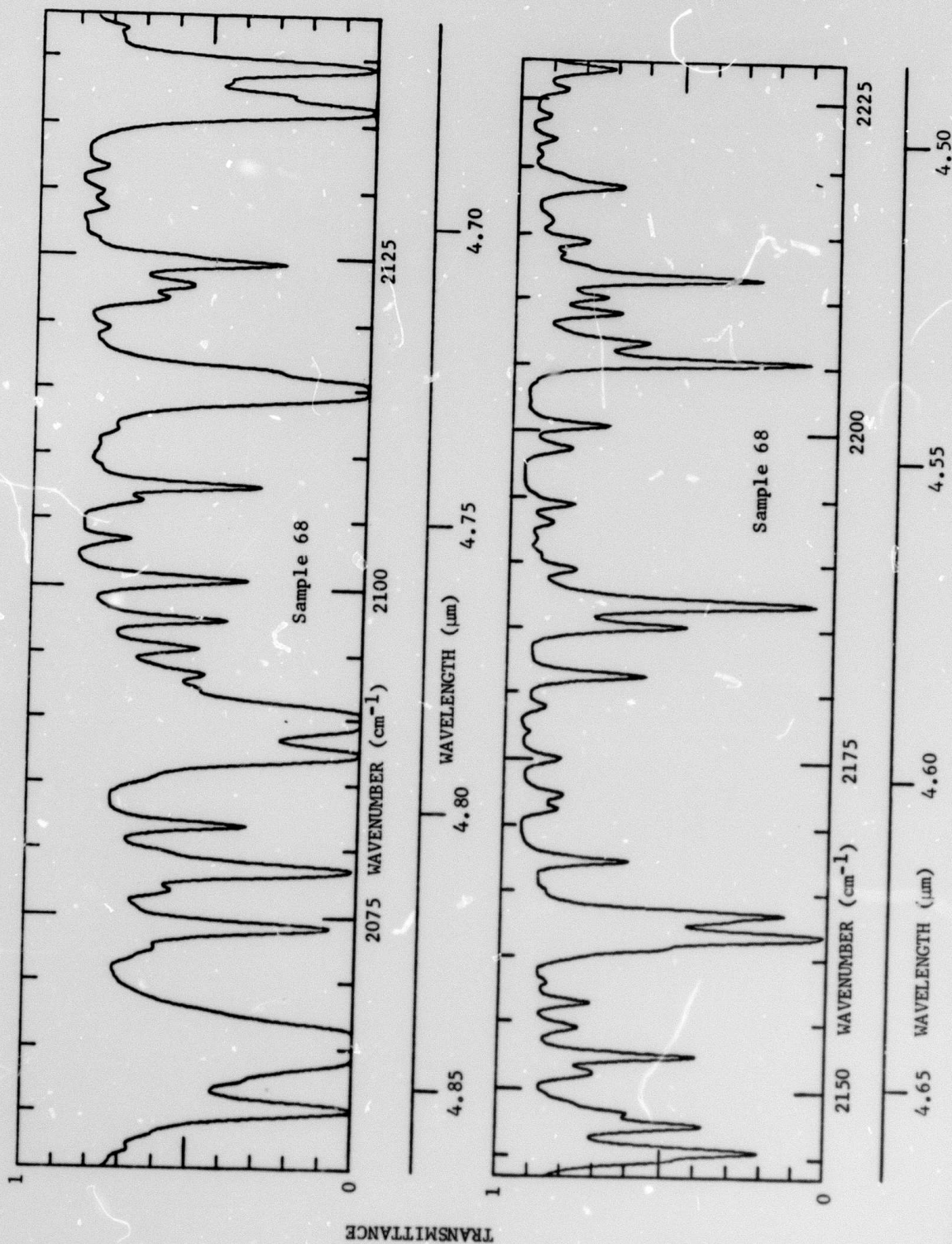


FIG.2-9. Spectral curve of transmittance between 2055 and 2230 cm^{-1} . Spectral slitwidth $\approx 0.3 \text{ cm}^{-1}$. Sample parameters are: 1 atm pure H_2O sample at 428K, 416 cm path length and $u = 71.4 \text{ E20 molecules/cm}^2$.

TABLE 2-1
INTEGRATED ABSORBANCE FOR PURE H₂O
 $\int_0^{\infty} \epsilon(\nu) d\nu \text{ (cm}^{-1}\text{)}$

Sample # (K)	33 428	34 428	68 428	68 428	18 322	25 322	25 322
P (atm)	0.2	0.05	0.05	0.05	0.0526	0.0167	0.0167
ν (molecules ⁻¹ cm ²)	113 E20	28.2 E20	3.58 E20	71.4 E20	114.0 E20	360 E20	360 E20
ν (cm ⁻¹)	ν (cm ⁻¹)	1840	1840	2056	1860	1860	1860
1840	0	0	0				
1845	5,000	3,866	2,124				
1850	9,993	7,708	3,915				
1855	14,494	8,899	4,142				
1860	19,216	10,927	4,831				
1865	24,143	13,235	5,649				
1870	29,132	17,184	7,808				
1875	33,650	18,921	8,399				
1880	37,807	20,453	8,957				
1885	41,639	21,452	9,241				
1890	46,385	23,734	10,199				
1895	51,301	25,947	10,822				
1900	55,643	27,766	11,597				
1905	59,723	29,046	11,990				
1910	64,192	30,933	12,736				
1915	68,674	32,359	13,137				
1920	73,637	35,334	14,307				
1925	78,591	38,111	15,470				
1930	81,984	38,708	15,600				
1935	85,467	39,739	15,907				
1940	89,349	40,709	16,119				
1945	94,293	43,572	17,382				
1950	98,411	45,176	17,971				
1955	101,280	45,915	18,199				
1960	105,054	47,164	18,540				
1965	108,188	47,882	18,722				
1970	112,821	50,150	19,534				
1975	114,759	50,470	19,572				
1980	116,734	50,927	19,644				
1985	119,222	51,538	19,744				
1990	123,065	52,801	20,141				
1995	127,637	55,122	21,163				
2000	130,411	55,783	21,325				
2005	132,262	56,166	21,382				
2010	135,225	57,006	21,630				
2015	137,267	57,351	21,686				
2020	141,876	59,518	22,516				
2025	144,722	60,184	22,729				
2030	146,900	60,808	22,875				
2035	148,382	61,161	22,959				
2040	150,355	61,551	23,066				
2045	154,103	62,837	23,595				
2050	155,888	62,264	23,724				
2055	157,413	63,602	23,778				
2060	158,344	63,718	23,813				
2065	161,290	64,581	24,115				
2070	163,801	65,591	24,495				
2075	163,801	65,591	24,495				
2080	163,801	65,591	24,495				
2085	163,801	65,591	24,495				
2090	163,801	65,591	24,495				
2095	163,801	65,591	24,495				
2100	163,801	65,591	24,495				
2105	163,801	65,591	24,495				
2110	163,801	65,591	24,495				
2115	163,801	65,591	24,495				
2120	163,801	65,591	24,495				
2125	163,801	65,591	24,495				
2130	163,801	65,591	24,495				
2135	163,801	65,591	24,495				
2140	163,801	65,591	24,495				
2145	163,801	65,591	24,495				
2150	163,801	65,591	24,495				
2155	163,801	65,591	24,495				
2160	163,801	65,591	24,495				
2165	163,801	65,591	24,495				
2170	163,801	65,591	24,495				
2175	163,801	65,591	24,495				
2180	163,801	65,591	24,495				
2185	163,801	65,591	24,495				
2190	163,801	65,591	24,495				
2195	163,801	65,591	24,495				
2200	163,801	65,591	24,495				
2205	163,801	65,591	24,495				
2210	163,801	65,591	24,495				
2215	163,801	65,591	24,495				
2220	163,801	65,591	24,495				
2225	163,801	65,591	24,495				
2230	163,801	65,591	24,495				
2235	163,801	65,591	24,495				
2240	163,801	65,591	24,495				
2245	163,801	65,591	24,495				
2250	163,801	65,591	24,495				
2255	163,801	65,591	24,495				
2260	163,801	65,591	24,495				
2265	163,801	65,591	24,495				
2270	163,801	65,591	24,495				
2275	163,801	65,591	24,495				
2280	163,801	65,591	24,495				
2285	163,801	65,591	24,495				
2290	163,801	65,591	24,495				
2295	163,801	65,591	24,495				
2300	163,801	65,591	24,495				
2305	163,801	65,591	24,495				
2310	163,801	65,591	24,495				
2315	163,801	65,591	24,495				
2320	163,801	65,591	24,495				
2325	163,801	65,591	24,495				
2330	163,801	65,591	24,495				
2335	163,801	65,591	24,495				
2340	163,801	65,591	24,495				
2345	163,801	65,591	24,495				
2350	163,801	65,591	24,495				
2355	163,801	65,591	24,495				
2360	163,801	65,591	24,495				
2365	163,801	65,591	24,495				
2370	163,801	65,591	24,495				
2375	163,801	65,591	24,495				
2380	163,801	65,591	24,495				
2385	163,801	65,591	24,495				
2390	163,801	65,591	24,495				
2395	163,801	65,591	24,495				
2400	163,801	65,591	24,495				
2405	163,801	65,591	24,495				
2410	163,801	65,591	24,495				
2415	163,801	65,591	24,495				
2420	163,801	65,591	24,495				
2425	163,801	65,591	24,495				
2430	163,801	65,591	24,495				
2435	163,801	65,591	24,495				
2440	163,801	65,591	24,495				
2445	163,801	65,591	24,495				
2450	163,801	65,591	24,495				
2455	163,801	65,591	24,495				
2460	163,801	65,591	24,495				
2465	163,801	65,591	24,495				
2470	163,801	65,591	24,495				
2475	163,801	65,591	24,495				
2480	163,801	65,591	24,495				
2485	163,801	65,591	24,495				
2490	163,801	65,591	24,495				
2495	163,801	65,591	24,495				
2500	163,801	65,591	24,495				
2505	163,801	65,591	24,495				
2510	163,801	65,591	24,495				
2515	163,801	65,591	24,495				
2520	163,801	65,591	24,495				
2525	163,801	65,591	24,495				
2530	163,801	65,591	24,495				
2535	163,801	65,591	24,495				
2540	163,801	65,591	24,495				
2545	163,801	65,591	24,495				
2550	163,801	65,591	24,495				
2555	163,801	65,591	24,495				
2560	163,801	65,591	24,495				
2565	163,801	65,591	24,495				
2570	163,801	65,591	24,495				
2575	163,801	65,591	24,495				
2580	163,801	65,591	24,495				
2585	163,801	65,591	24,495				
2590	163,801	65,591	24,495				
2595	163,801	65,591	24,495				
2600	163,801	65,591	24,495				
2605	163,801	65,591	24,495				
2610	163,801	65,591	24,495				
2615	163,801	65,591	24,495				
2620	163,801	65,591	24,495				
2625	163,801	65,591	24,495				
2630	163,801	65,591	24,495				
2635	163,801	65,591	24,495				
2640	163,801	65,591	24,495				
2645	163,801	65,591	24,495				
2650	163,801	65,591	24,495				
2655	163,801	65,591	24,495				
2660	163,801	65,591	24,495				
2665	163,801	65,591	24,495				
2670	163,801	65,591	24,495				
2675	163,801	65,591	24,495				
2680	163,801	65,591	24,495				
2685	163,801	65,591	24,495				
2690	163,801	65,591	24,495				
2695	163,801	65,591	24,495				
2700	163,801	65,591	24,495				
2705	163,801	65,591	24,495				
2710	163,801	65,591	24,495				
2715	163,801	65,591	24,495				
2720	163,801	65,591	24,495				
2725	163,801	65,591	24,495				
2730	163,801	65,591	24,495				
2735	163,801	65,591	24,495				
2740	163,801	65,591	24,495				
2745	163,801	65,591	24,495				
2750	163,801	65,591	24,495				
2755	163,8						

SECTION 3

CONTINUUM ABSORPTION

Two different methods were used to obtain data on the continuum for self-broadening in the narrow windows. In the first method, a sample of H_2O vapor was placed in the cell and several narrow spectral intervals containing a window were scanned. Additional H_2O was added and the narrow intervals were re-scanned. The process was repeated for 3 to 5 pressures, requiring approximately four hours for a series of measurements. In the second method a single narrow interval was studied at a time. The sample was added to its maximum pressure as quickly as possible and the transmittance was measured. Transmittance was measured at four or five pressures as the pressure was decreased, with about 20 minutes required to make the series of measurements over a single interval. Data obtained by the second method were more self-consistent than the others. The results obtained by the two methods did not agree as well as expected, although the discrepancies were smaller than those observed in a previous study of the $2400\text{-}2900\text{ cm}^{-1}$ region.

Only the first method was practical for samples contained in the large absorption cell. The cell is so large that it takes a lot of H_2O and a long time to introduce a sample. The large vacuum pump used with the long cell vibrates the cell so that the mirrors must be readjusted each time the pump is operated. It is difficult to exactly duplicate the previous alignment, so it is impractical to use the same background curve for different samples obtained by removing a portion of the previous sample. Therefore, samples were changed by adding H_2O to the previous one. Only 7 short spectral intervals were scanned by this method when using the long cell. The scans were repeated a few times for each sample to allow averaging. Several of the measurements were repeated by evacuating the cell and introducing a new H_2O sample.

The second method was used for samples contained in the small multiple-pass cell. The cell is small enough that only a few minutes are required to fill the cell. The pump used to evacuate the cell is connected to it by rubber tubing and does not cause vibrations that affect the optical alignment.

Determining the continuum coefficients for pure H₂O involved the application of Eqs. (1-2) and (1-5) to transmittance values observed at the points of maximum transmittance in the short spectral interval scans. We plotted values of $(-1/u) \ln T$ at a given wavenumber versus p for a fixed temperature and path length. In accordance with the discussion of Eq. (1-5), we expect the plotted points to fall on a straight line that intersects the $p = 0$ line at $\kappa(\text{local})$ and has a slope equal to C_g^0 . Two typical plots are shown in Fig. 3-1 for 1978.6 cm⁻¹. This wavenumber is very close to one of the CO laser lines studied by Long et al.² The straight line fits the points well and passes near the origin. This result is expected for continuum absorption with little contribution due to local lines. Similar results were obtained at other wavenumbers and for samples at other temperatures.

Values of the continuum coefficient, C_g^0 , for self-broadening are listed in Table 3-1 for four different temperatures and several wavenumbers. The symbol L adjacent to some of the wavenumber listings indicates that some local-line absorption had to be accounted for in order to determine the continuum coefficient at that position. The 322 K samples were contained in the long absorption cell; the others were in the short cell. A long path length was needed at 322 K in order to produce a measurable absorptance because the maximum H₂O pressure was limited to approximately 0.07 atm by the H₂O vapor pressure.

Several factors contribute to the errors in the results. One of the most important is the error in the assumed 100% transmittance curves (background). This error is obviously most serious when the absorptance is small. Noise, or short term fluctuations, also contribute. Additional uncertainty arises from errors in accounting for the local line absorption and the influence of the finite slitwidth of the spectrometer. The estimated errors are $\pm 5\%$ for the majority of the values listed in Table 3-1. These results were obtained from plots of $(-1/u) \ln T$ vs p that contain several points. Values of C_g^0 in the table with an estimated error of $\pm 10\%$ result from either of two types of data. Some result from plots of $(-1/u) \ln T$ vs p with considerable scatter, or with only two or three points. Other values are based on the transmittance curves shown in Section 2. The majority of the values listed for 322 K were obtained from the transmittance curves of Samples 25 and 18.

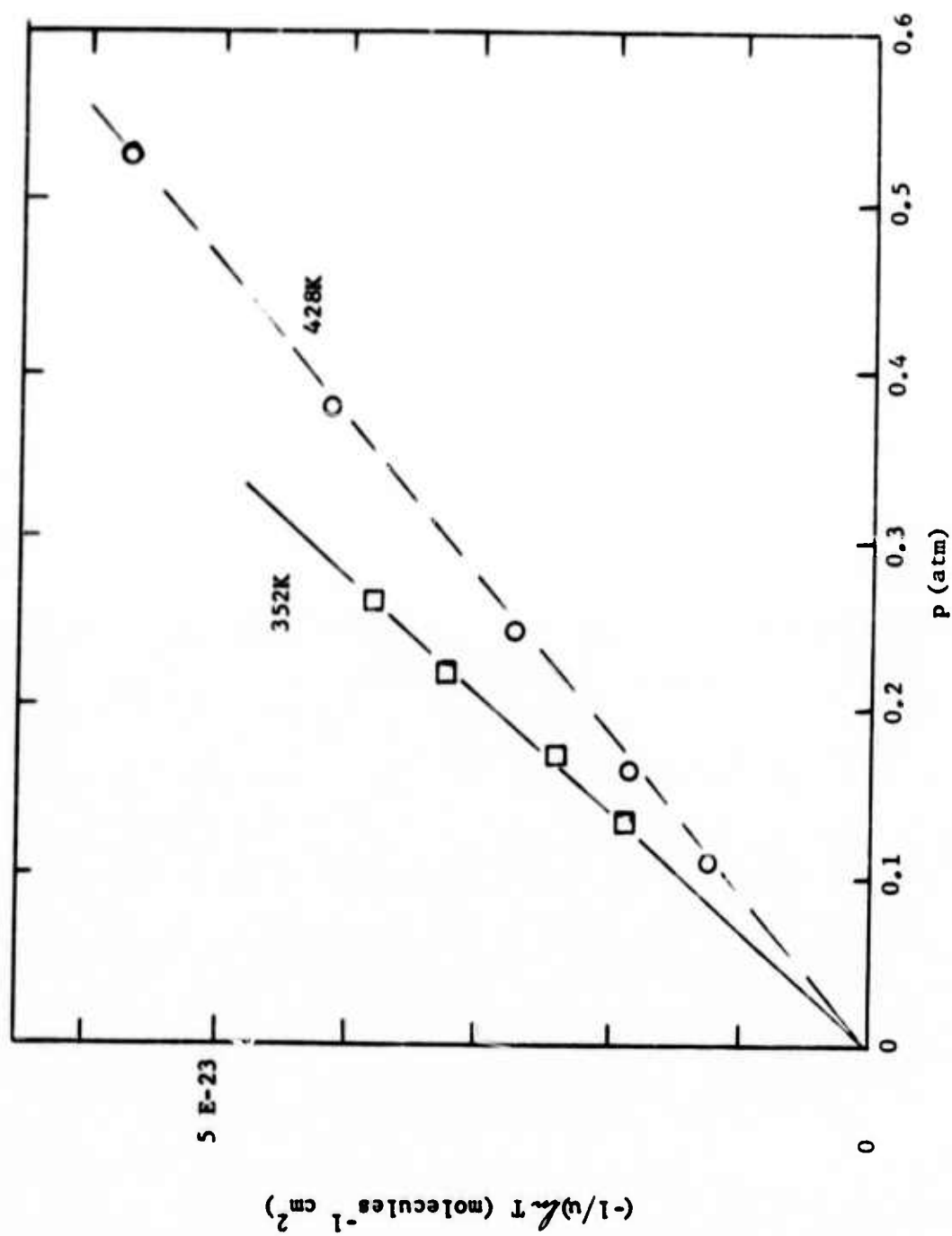


FIG. 3-1. Plots of $(-1/u)\Delta T$ vs p at 1978.6 cm^{-1} for H_2O at 352 K and 428 K.

TABLE 3-1

SELF-BROADENING AND N₂ BROADENING COEFFICIENTS FOR DIFFERENT TEMPERATURES

ν cm ⁻¹	Multiply all values by 10 ⁻²⁴ molecules ⁻¹ cm ² atm ⁻¹						$B = C_B^0/C_{N_2}^0$		
	C_B^0			$C_{N_2}^0$			428 K	353 K	308K
	428 K	353 K	322 K	308 K	428 K	353 K	308 K		
1630.5		5040		8640		871	1040	5.8	8.3
1665.5		6120		10000		1100	1360	5.6	7.4
1691.5		8410		11900		1500	1820	5.6	6.5
1725.2		4250		6770		696	723	6.1	9.4
1765.0		4570		5350		695	688	6.6	7.8
1786.5		2810		3420		419	425	6.7	8.1
1814.5		1490		1890		195	190 *	7.7	9.9
1839.8		1780		2160		283	297 *	6.3	6.9
1854.6 L	583	845				90		9.3	
1882.0 L	419	560	724 *		83.1	58		7.0	
					57.0			7.3	
1900.0	371		619 *					6.5	
1905.6	488	600	808 *		84.5	91.5		5.8	6.6
1920.5	1640		1900 *		296			5.5	
1927.1	433		654 *						
1929.2	281	342	478 *		42.9	41.0		6.6	8.4
1931.3	285	372	488 *						
1948.2	344		514 *		46.4	37.7 *		6.2	9.9
1952.6 L	199	247	284						
1959.0	222		342 *		29.7	26.3 *		6.7	9.4
1962.8	238	283	392 *			39.5 *			7.2
1974.0	118		204		16.7			7.1	
1978.5	108	144	190 *		13.7	12.5 *		7.9	11.5
1983.8 L	139		218 *						
1990.0 L	766		905 *		159			4.8	
1997.4	164		222 *		27.5			6.0	
2002.3 L	93.1		157 *						
2006.4 L	139		172 *						
2008.8 L	272		330 *						
2011.8 L	122		172 *						
2029.3	61.8	77.7	105 *			6.2 *			12.5
2036.1	80.7		110 *		12.2			6.6	
2045.3	125		137 *						
2055.5	40.4		72.5 *		5.55 *			7.3	
2056.0	39.1		74.8						
2071.1	43.1	52	70.5 *		6.65 *	4.5 *		6.5	11.5
2083.6 L	37.8	42.5	59.3 *			3.8 *			11.2
2102.4 L	20.2		35.0						
2109.6 L	22.6		47.9 *		3.0 *			7.5	
2130.7 L	18	20	37.1 *		1.9 *	1.7 *		9.5	11.8
2133.0	21.1		38.2						
2169.8	8.8		25.1 *		1.2 *			7.3	
2196.7	7.0	11.8 *	23.2 *		.86 **	0.58 **		8.1	20
2223.3 L	7.9		20						
2290.0			17.9						

Estimated errors for C_B^0 and $C_{N_2}^0$ are $\pm 5\%$ except for values marked * and ** which indicate $\pm 10\%$ and $\pm 20\%$, respectively. Errors in B depend on the associated values of C_B^0 and $C_{N_2}^0$.

Influence of Nitrogen-Broadening on the Continuum

The earth's atmosphere contains much more N_2 and O_2 than H_2O so that the broadening of H_2O lines by N_2 and O_2 is generally more important than the self-broadening. Furthermore, the N_2 concentration is approximately 4 times that of O_2 and the continuum coefficient $C_{O_2}^0$ is not expected to be greatly different from $C_{N_2}^0$. Therefore, $C_{N_2}^0$ can probably be used for air in the place of a more accurate weighted average of $C_{N_2}^0$ and $C_{O_2}^0$. No data were obtained with O_2 .

In a typical measurement of $C_{N_2}^0$ the spectrometer was adjusted to one of the narrow windows where the N_2 continuum absorption dominates over the local-line absorption. A sample of H_2O was added to the cell until the transmittance dropped to about 80%. A spectrum was scanned over the window, and N_2 was added in steps to produce transmittance of about 60, 45, 30, and 20%. The transmittance was measured at each pressure after the sample had mixed for several minutes. The total operation for all the pressures required between 20 and 30 minutes for a single window. We plotted $(-1/u) (\ln T - \ln T')$ versus p_{N_2} , where T' is the transmittance of the pure H_2O sample. In accordance with Eq. (1-6) the points fell on a straight line drawn through the origin with a slope of $C_{N_2}^0$. The values obtained for three different temperatures are given in Table 3-1. The estimated errors for $C_{N_2}^0$ are as high as 20% at some wavenumbers because the increase in N_2 absorption resulting from the N_2 was very small. The large errors were assigned to the values that were determined from $(\ln T' - \ln T) < 0.05$. The three right-hand columns in Table 3-1 list values of $B = C_s^0 / C_{N_2}^0$ for three different temperatures.

In previous studies^{6,13} we have found B to occur between 4 and 6 at wavenumbers where most of the absorption is due to lines centered within 5 or 10 cm^{-1} . As can be seen in Table 3-1, values of B for the continuum may extend to higher values. The wider variation can probably be attributed to differences in the distances from the centers of the lines producing most of the absorption. At 1920.5 cm^{-1} , for example, where the strong nearby lines are responsible for most of the absorption, B has a relatively low value of 5.5. In contrast, no strong lines occur within several cm^{-1} of 1978.5 cm^{-1} ; therefore, a large fraction of the continuum at this point is probably due to lines centered more than 10 cm^{-1} away. The corresponding value of B is much larger, 7.9 at 428 K and 11.5 at 353 K.

Variations in B are shown graphically by the curves of transmittance in Fig. 3-2. Sample 42 consists of pure H_2O in the small multiple-pass cell adjusted for a path length of 8.26 meters. For Sample 45 the cell was adjusted to 32.9 meters, and 0.0486 atm of H_2O was introduced to match the absorber thickness of Sample 42; then N_2 was added to 0.5 atmospheres. To produce Sample 45, N_2 was added to Sample 45 to a total pressure of 1 atm. Portions of two of the curves have been omitted where

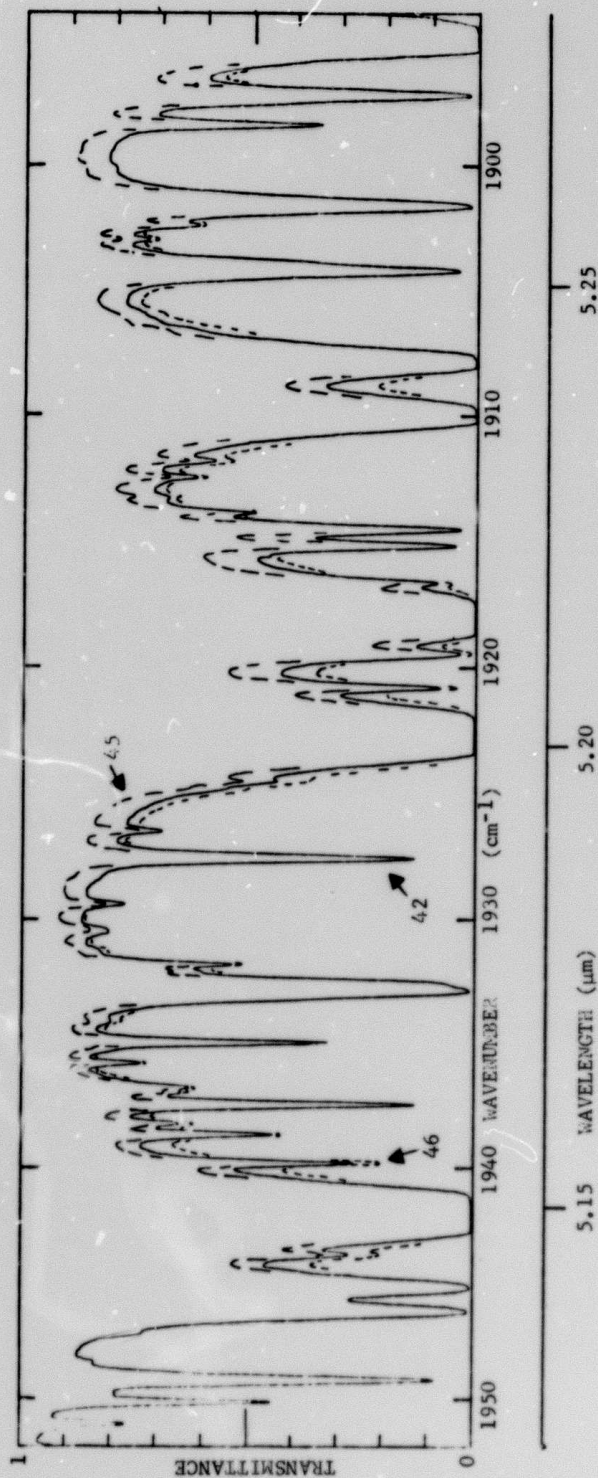


FIG. 3-2. Spectral curves showing a comparison of self-broadened and N_2 -broadened H_2O lines. Spectral Slitwidth = 0.19 cm^{-1} .

they are nearly coincident with the curve for Sample 42. All three samples have the same absorber thickness; therefore, any differences in the curves are due to differences in line width or shape. In the case of Sample 42 the lines are entirely self broadened, whereas the lines in Sample 45 and 46 are partially self broadened and partially N_2 broadened. If the N_2 -broadened lines had exactly the same shape as the self-broadened lines, we would be able to adjust the N_2 pressure in a sample such as Samples 45 or 46 so that its spectral curve was coincident with that of Sample 42. Inspection of Fig. 3-2 shows that this is not possible. For example, near 1900 and 1930 cm^{-1} , Sample 46 nearly matches Sample 42. By substituting the corresponding pressures in Eq. (1-7), we can show that this corresponds to $B = 6.5$. At the transmittance maxima near 1909 and 1919 cm^{-1} , the value of B found by interpolation is very close to 5. At other points within the spectral interval shown where the curves are not too steep to measure accurately, the corresponding values of B lie between about 5.0 and 6.5.

Data similar to those shown in Fig. 3-2 were obtained in other portions of the spectra. As indicated in Table 3-1, larger values of B were observed in some of the windows at higher wavenumbers. Generally $B \approx 5$ at places where most of the absorption can be attributed to lines centered within 5-10 cm^{-1} . The value of B is consistently greater than 5 at points where a large fraction of the continuum results from lines centered more than 10 cm^{-1} away. This result is consistent with previous work by Palmer¹⁴ in the 250-500 cm^{-1} region and with other work^{4,5,7,15} in the 8-12 μm window and the 4 μm window.

The variation in B can be explained on the basis of a difference in the shapes of the extreme wings of N_2 -broadened and self-broadened H_2O lines. Within about 5 or 10 cm^{-1} of the centers, both types of lines apparently have similar shapes with the normalized half-width α^0 about 5 times as great for self-broadened lines as for N_2 -broadened ones. However, beyond 5 or 10 cm^{-1} from the centers, the absorption by self-broadened lines relative to N_2 -broadened ones is apparently greater than it is near the centers. This corresponds to a larger value of χ (in Eq.(1-4)) for the wings of self-broadened H_2O lines than for N_2 -broadened lines.

Values of C_s^0 at a given wavenumber are seen from Table 3-1 to decrease with increasing temperature. The temperature dependence generally cannot be explained by changes in the intensities and widths of the lines. Line widths decrease with increasing temperature, but not at sufficiently fast rate to account for the changes in C_s^0 . Throughout most of the spectral region studied, the intensities of the lines increase with increasing temperature, an effect opposite to that required to explain the temperature dependence of C_s^0 . The most probable explanation is a change in the shapes of the wings of the lines that can be represented by a decrease in χ with increasing temperature. The largest

relative changes in C_s^O occur at wavenumbers where a significant portion of the absorption is due to distant lines. Thus, we conclude that the relative temperature dependence of χ increases with increasing $|\nu - \nu_0|$.

At most of the wavenumbers investigated, $C_{N_2}^O$ also decreases with increasing temperature. At those places where N_2 this does not occur, the dependence can probably be explained by the increased intensities of the lines producing the absorption. The results generally indicate that χ for N_2 -broadened lines also decreases with increasing temperature, but at a slower rate than self-broadened lines. This accounts for the decrease in B with increasing temperature.

Long et al.² have measured the absorption coefficients at several wavenumbers for relatively dilute samples of H_2O in N_2 at 1 atm total pressure. Their experimental values are from about 1.2 to 3 times as great as values calculated by using the line parameters of Benedict and Calfee¹ and the Lorentz line shape. The ratio of the experimental to the calculated values is generally less at points where the nearby lines ($|\nu - \nu_0| < 10 \text{ cm}^{-1}$) contribute most of the absorption than it is at points where the absorption is due primarily to distant lines. At wavenumbers where direct comparisons can be made with room temperature data, we find good agreement between our values and the results of Long et al. At other wavenumbers where we have data only at elevated temperatures, we extrapolated curves of C_s^O and $C_{N_2}^O$ to room temperature and, again, found good agreement with Long et al.² These results imply that the wings of N_2 -broadened H_2O lines are "super-Lorentzian"; i.e., they absorb more than Lorentz lines having the same intensities and widths. ($\chi > 1$ in Eq. (1-4).)

In summary, the results indicate that χ is greater for the wings of self-broadened H_2O lines than for N_2 -broadened ones, and that it is greater than unity for both types at the temperatures studied. Furthermore, the ratio of χ for self-broadened lines to that for N_2 -broadened ones increase with increasing distance from the line centers and with decreasing temperature.

SECTION 4

REFERENCES

1. W. S. Benedict and R. F. Calfee, ESSA Professional Paper 2, June 1967.
2. R. K. Long, F. S. Mills, G. L. Trusty, and D. F. Ford, Oral Paper presented at the Fall Meeting of the Opt. Soc. Am., October 1972.
3. D. K. Rice, "Absorption Measurements of Carbon Dioxide Laser Radiation by Water Vapor," Northrop Corporation Report #NLSD72-11R, Contract No. N00014-72-C-0043, ARPA Order #1806, July 1972.
4. K. J. Bignell, F. Saiedy, and P. A. Sheppard, J. Opt. Soc. Am. 53, 446 (1963).
5. K. J. Bignell, Quart. J. Roy. Met. Soc. 96, 390 (1970).
6. D. E. Burch, D. A. Gryvnak, and J. D. Pembroke, "Investigation of the Absorption of Infrared Radiation by Atmospheric Gases: Water, Nitrogen, Nitrous Oxide," Aeronutronic Report U-4897, Contract No. F19628-69-C-0263, January 1971.
7. D. E. Burch, Philco-Ford Publication U-4784, Contract No. F19628-69-C-0263, January 1970.
8. D. E. Burch, D. A. Gryvnak, R. R. Patty, and Charlotte Bartky, "The Shapes of Collision-Broadened CO₂ Absorption Lines," Aeronutronic Report U-3203, Contract NOnr 3560(00), 31 August 1968.
9. B. H. Winters, S. Silverman, and W. S. Benedict, J. Quant. Spectry Radiative Transfer 4, 527 (1964).
10. D. E. Burch, D. A. Gryvnak, and J. D. Pembroke, "Investigation of the Absorption of Infrared Radiation by Atmospheric Gases," Aeronutronic Report U-4829, Contract No. F19628-69-C-0263, June 1970.
11. P. Varanasi, S. Chou, and S. S. Penner, J. Quant. Spectry Radiative Transfer 8, 1537 (1968).
12. W. S. Benedict, H. H. Claassen, J. H. Shaw, J. Research Nat'l Bur. Standards, Vol. 49, No. 2, 91 (1952).

REFERENCES (Cont.)

13. D. E. Burch and D. A. Gryvnak, "Absorption by H₂O Between 5045-14,485 cm⁻¹ (0.09-1.98 microns)," Aeronutronic Report U-3704, Contract No. NONr 3560(00), ARPA Order No. 237, Amendment #23/1-3-66, July 1966.
14. C. H. Palmer, Jr., J. Opt. Soc. Am. 50, 1232 (1960).
15. R. K. Long, J. H. McCoy, D. B. Rensch, Appl. Opt. 8, 1471 (1969).